
ORIGINAL ARTICLE

Bipolar Radiofrequency Lesion Geometry: Implications for Palisade Treatment of Sacroiliac Joint Pain

Eric R. Cosman, Jr., PhD*; Christian D. Gonzalez, MD, FIPP[§]

**Cosman Medical, Inc., Burlington, Massachusetts; [§]Department of Anesthesiology, University of Massachusetts, Worcester, Massachusetts, U.S.A.*

■ **Abstract:** Ex vivo photographic temperature mapping of bipolar radiofrequency (RF) lesions in animal tissue is performed over a wide range of electrode tip spacings, tip lengths, tip diameters, tip temperatures, and lesion times. In vivo temperature measurements collected during clinical treatment of sacroiliac joint (SIJ) pain corroborate those collected ex vivo. Generation of a "strip lesion" connecting two separated bipolar electrode tips is demonstrated ex vivo for tip spacings as large as 20 mm. A rounded rectangular bipolar lesion with midline dimensions 12 mm × 15 mm × 8 mm (L × W × D) is demonstrated using 10 mm parallel tip spacing, 10 mm tip lengths, 20 gauge cannulae, 90°C tip temperature, and 3-minute lesion time. Lesion length can be increased to 18 mm by using 15 mm tip lengths. Lesion width can be increased to 17 mm by using 12 mm tip spacing. The size of conventional bipolar lesions can exceed the size of lesions produced both by conventional monopolar RF (12 mm × 7 mm × 7 mm ellipsoidal) and by

cooled monopolar RF as used in spinal pain management (10 mm × 10 mm × 10 mm spherical). SIJ pain is treated by placing 5 to 7 straight RF cannulae perpendicular to the dorsal sacrum and producing 4 to 6 overlapping bipolar RF lesions between the dorsal sacral foramina and the ipsilateral SIJ. This bipolar "palisade" (a defensive fence) creates a continuous lesion spanning the region through which multiple sacral lateral branch nerves travel along irregular, branching paths to reach the SIJ. ■

Key Words: bipolar radiofrequency lesion size, bipolar RF electrode spacing, sacroiliac joint pain treatment, back pain management

INTRODUCTION

The sacroiliac joint (SIJ) is reportedly involved in 15 to 25% of cases of axial lower back pain.¹ Referred pain due to SIJ dysfunction commonly radiates into the buttocks, lumbar region, and lower extremity. Conservative treatment of SIJ pain primarily involves medical management, with little benefit from physical therapy. Steroidal injections into the SIJ have been performed for decades, though evidence of their long-term benefit is mixed. More recently, radiofrequency (RF) lesioning of the joint's dorsal innervations has been proposed as a means to extend the duration pain relief and to avoid the cumulative side effects of corticosteroids. RF treatment can be clinically effective, but is complicated by

Address correspondence and reprint requests to: Eric R. Cosman Jr., PhD, 76 Cambridge Street, Burlington, MA 01803, U.S.A. E-mail: ercosman@alum.mit.edu.

Disclosures: Eric Cosman, Jr. is employed by Cosman Medical, Inc., Burlington, MA. This research was financially supported by Cosman Medical, Inc. in the form of equipment. Christian Gonzalez is employed by UMass Memorial Hospital, Worcester, MA; has no financial interest in Cosman Medical, Inc.; and is not funded by Cosman Medical, Inc.

Submitted: February 1, 2010; Revision accepted: April 29, 2010

DOI: 10.1111/j.1533-2500.2010.00400.x

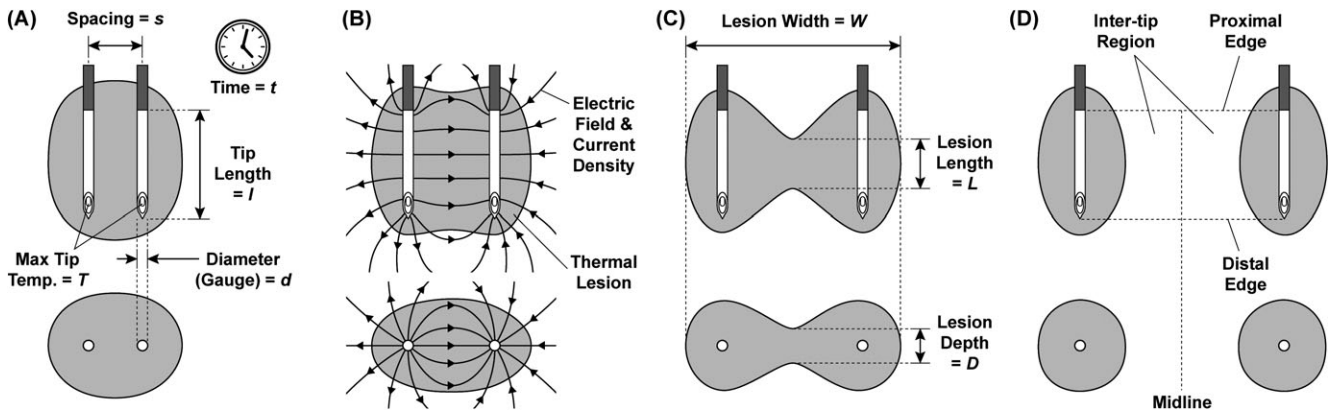


Figure 1. (A) For parallel-electrode configurations, bipolar RF lesion geometry depends on the parameters: electrode tip spacing s , tip length l , tip diameter/gauge d , maximum tip temperature T , and lesion time t . (B) The electric and current density fields are focused between closely-spaced bipolar electrodes, preferentially heating the inter-tip region. (C) Bipolar lesion size and inter-tip connectivity can be characterized by the lesion's midline length L , width W , and midline depth D . (D) The "inter-tip" region is the area between the uninsulated tips of two electrodes. (A–D) Each panel shows a bipolar thermal lesion in lateral (top) and needle (bottom) views. As tip spacing s increases, the lesion expands in width W and narrows in both length L and depth D at the midline. The range of spacing values s over which this transition occurs depends on the other configuration parameters l , d , T , and t .

the need to target multiple lateral branch nerves arising from S1, S2, S3, and perhaps S4, which have been shown to follow irregular, branching paths to the SIJ.²

Clinicians have tried to overcome this complication by using bipolar RF electrode configurations to create larger lesions than can be created with monopolar RF.^{3,4} Whereas a monopolar configuration drives RF current between an electrode's exposed tip and a distant ground pad, a bipolar configuration drives RF current between two nearby electrode tips. As bipolar electrode tips are brought closer together, the resulting thermal lesion shape transitions from that of two volumes surrounding each tip separately, to that of a single volume connecting the tips. Figure 1 illustrates this shape transition for a bipolar configuration in which the energized tips are on separated, parallel probes. The connected geometry and larger total lesion volume are strongly influenced by a focusing of the electric and current density fields between closely-spaced electrode tips. Higher RF electric fields and current densities induce more rapid tissue heating, and the resulting lesion temperature distribution is influenced by heat-conduction and blood-flow dynamics.^{5,6} For larger tip spacings, the focusing effect is less pronounced, and the electric and current density fields approach the distribution of two independent monopolar electrodes that are referenced to a distant dispersive ground pad.

While monopolar RF has been used widely in neurosurgery and pain management since the earliest RF lesion generators were built by B. J. Cosman, S. Aranow,

and O. A. Wyss in the early 1950s,^{7–9} bipolar RF has been used less frequently and is less well understood. The only two pertinent studies of bipolar lesion geometry were conducted ex vivo in chicken egg white, and together addressed electrodes of only two sizes: a dorsal root entry zone electrode whose tip has 31 gauge (0.25 mm) diameter and 2 mm length,¹⁰ and a spinal cannula/electrode whose tip has 22 gauge diameter and 5 mm length.¹¹ Given the limited scope of these studies and substantial physical differences between fluid egg white and solid animal tissue, many technical questions about the geometry of bipolar RF lesions remain unanswered. How does lesion size depend on the spacing between bipolar tips, active tip length, cannula diameter, set temperature, and lesion time? What combination of these parameters can efficiently and reliably create lesions suited to target anatomy? What placement techniques can a clinician use to facilitate treatment and improve outcomes? Answering these questions is critical to evaluating the use of bipolar RF in previous clinical applications and to optimizing its use in the future.

In this study, both in vivo and ex vivo temperature mapping show how bipolar lesion shape varies over a wide range of geometric and RF parameters. This information is translated into a straightforward clinical method for lesioning the dorsal SIJ innervation that is designed to create a more complete lesion zone than previous methods. In particular, a row of straight RF cannulae are placed perpendicular to the dorsal sacrum to produce contiguous bipolar RF lesions between the

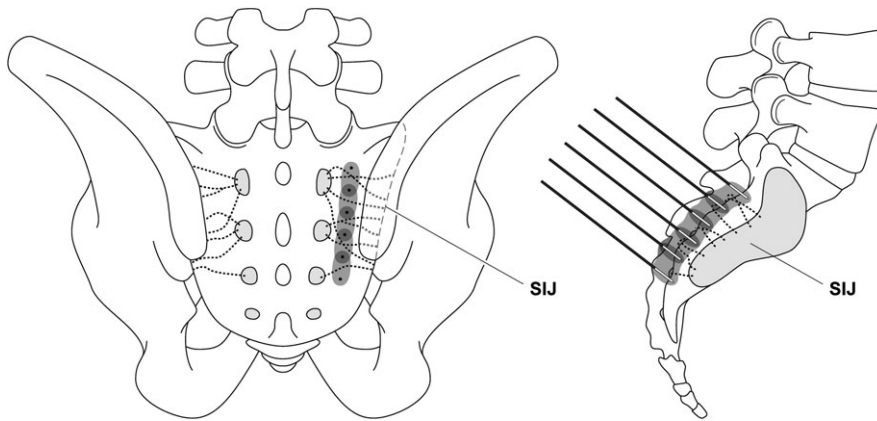


Figure 2. Palisade treatment of sacroiliac joint pain. A row of straight RF cannulae are inserted to contact the dorsal sacral surface perpendicularly between the S1–S3 foramina and the SIJ line. Bipolar RF lesions generated between adjacent cannulae produce a continuous palisade lesion across the region where sacral lateral branch nerves (dotted lines) travel from the sacral foramina to the SIJ. (Left) Needle view. (Right) Lateral view.

dorsal sacral foramina and the sacroiliac joint line (Figure 2). By analogy to a defensive fence, this bipolar “palisade” is intended to create a continuous heat lesion that spans the entire region through which the sacral lateral branch nerves travel to the SIJ.

METHODS

Ex Vivo Data Collection

The experimental setup for ex vivo data collection in bovine liver is shown in Figure 3. Two straight, sharp RF cannulae (CC10xx, Cosman Medical, Burlington, MA, U.S.A.) and a 29-gauge (0.33 mm diameter) cordotomy electrode (Cosman LCE) are anchored together to constrain the spacing between the uninsulated cannula tips and the position of the cordotomy electrode. These anchored elements are placed on top of a lower slab of adult bovine liver whose top surface is cut flat. A second cordotomy electrode is inserted through the top surface of the lower liver slab to fix its position relative to the other elements. An RF electrode (Cosman CSK-TC10) is placed within each cannula to electrify its uninsulated tip and to monitor its temperature. The RF electrodes are attached to outputs 1 and 2 of a four-output radiofrequency generator (Cosman G4). The cordotomy electrodes' thermocouple wires are connected to outputs 3 and 4 of the RF generator, but their RF wires are left disconnected so that they serve only as electrically-passive, fine-gauge, remote temperature probes. As shown in Figures 4A and 4B, these probes are placed at the center of the inter-tip region and at the center of the distal-edge of the inter-tip region because these midline temperatures are indicative of lesion geometry. A second slab of adult bovine liver is placed on top of the first slab, and the two slabs are

pressed together firmly so that the cannulae/electrodes and remote temperature probes are surrounded by tissue. The RF generator produces a bipolar lesion by driving RF current between the tips of the RF cannulae, automatically adjusting the output level so that neither electrode's tip exceeds a target temperature, and so that at least one electrode's tip is held within $\pm 2^\circ\text{C}$ of that target temperature for a specified lesion time. The target temperature is achieved within approximately 15 seconds. The G4 generator stores measurements once per second, including electrode tip temperatures, remote probe temperatures, inter-electrode impedance, RMS voltage, RMS current, and average power output. After the lesion is complete, the top liver slab is removed and a photograph (Canon EOS 20D, Canon USA Inc., Lake Success, NY, USA; Canon EF 100 mm f/2.8 Macro Lens) is taken perpendicular to the bottom slab to document the cross-sectional length and width of the lesion. In some configurations, the lesion in the lower slab is cut in half, perpendicular to electrode direction, and half of the lesion's depth dimension is measured.

Bipolar lesions are created by varying the configuration parameters shown in Figure 1A: inter-tip spacing s , cannulae diameter d , tip lengths l , tip temperature T , and lesion time t . Inter-tip angle (Figure 5A) and inter-tip offset (Figure 5D) are also varied. Spacing is measured between the central axes of the cannulae to ± 1 mm accuracy before heating, because tissue can contract in the heating process. Sampling of this large parameter space is centered on the base configuration 10 mm parallel spacing, 20 gauge diameter, 10 mm tip length, 90°C set temperature, and 3-minute lesion time. As each parameter is varied, the base configuration is repeated in multiple samples of bovine liver to establish variability in lesion size estimates.

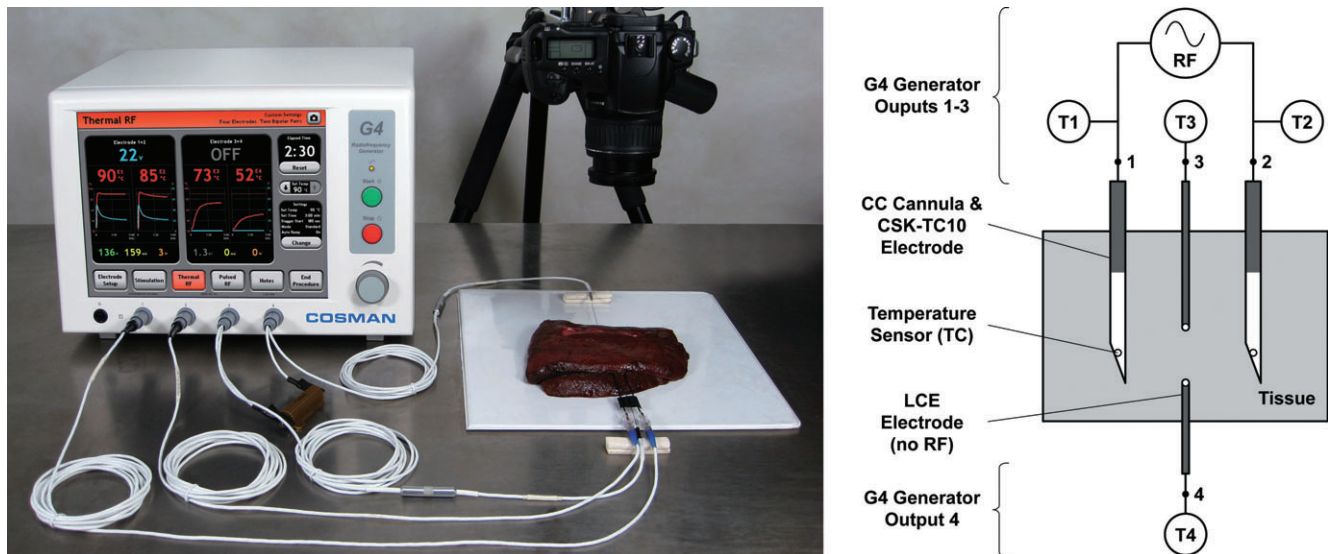


Figure 3. Experimental setup for ex vivo animal tissue data collection.

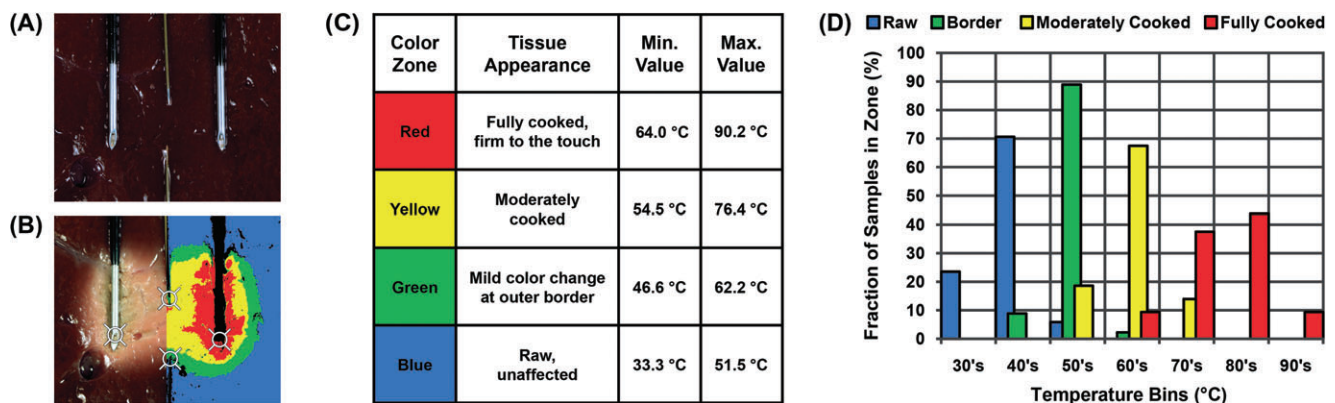


Figure 4. Ex vivo photographic temperature mapping. (A, B) Pre- and post-lesion photographs for a bipolar RF configuration in ex vivo beef liver. Crosshairs indicate the locations of remote and intra-tip thermocouples. The right half of the post-lesion photograph shows the quantization of RGB pixel values into four color zones. Unclassified pixels are colored black. (C, D) The minimum, maximum, and histogrammed distribution of temperatures measured in each color zone at the end of 3-minute lesions in ex vivo beef liver. These statistics are based on a total of 154 thermocouple measurements.

The same setup is used with samples of bovine muscle, chicken muscle, and porcine muscle to demonstrate consistency or variability of lesion geometry across animal tissues. A similar setup is also used in which cannula are suspended in chicken egg white, to allow for direct comparison with a previous study of bipolar lesion geometry.¹¹ Adult bovine liver is selected as the primary media for this investigation because preliminary temperature measurements indicated that its color begins changing between about 45°C to 50°C (see Figure 4). In contrast, egg white and the muscles were observed to change color at higher temperatures, reducing the visible extent of thermal heating patterns. The use of solid tissue also

eliminates questions about inhomogeneities and fluid convection that are known to exist in egg white.

Before a lesion is created, the tissue or egg white is covered with a plastic sheet to preserve moisture, and is allowed to equilibrate at room temperature (mode: 25°C, min: 18°C, max: 29°C). This is expected to produce conservative assessments of lesions size relative to those that might be produced when starting at body temperature 37°C. A small set of preliminary experiments were conducted in which the bovine liver and egg white media were pre-heated in a calibrated oven (Lindberg/Blue M, model M01450SA-1) set to 37°C, and no pronounced difference in lesion geometry was observed.

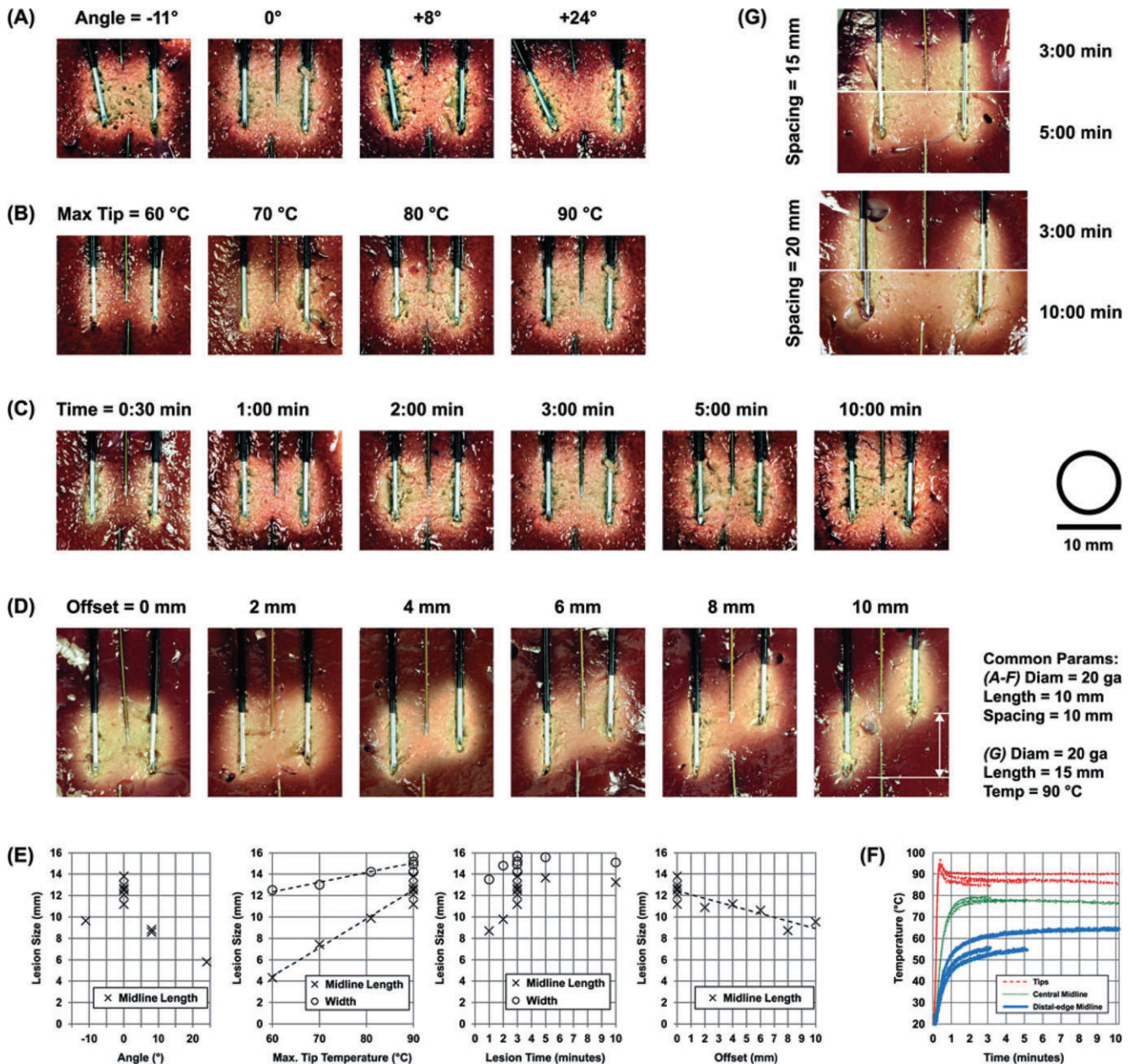


Figure 5. (A–D) Cross-sectional photographs of bipolar lesions in ex vivo adult bovine liver for variations in inter-tip angle, tip temperature, lesion time, and parallel inter-tip offset, starting from the base configuration 10 mm parallel spacing, 20 gauge diameter, 10 mm tip length, 90°C tip temperature, 3-minute lesion time. (E) Measurements of midline lesion length L and width W are based on the dimension of the moderately-cooked region (yellow color zone) measured in the photographs of panels A through D, among others. (F) Intra-tip and inter-tip temperature time-series collected during generation of the 3-, 5-, and 10-minute lesions shown in panel C. The higher variability in distal-edge midline temperature measurements is likely due to higher temperature gradients at that location. (G) The upper and lower half of each image compares different lesion times for a bipolar configuration with 15 mm tip lengths, 20 gauge diameter, and 90°C tip temperature. Inter-tip lesion size continues to increase substantially after 3 minutes for the 20 mm spacing (bottom), whereas it has saturated by 3 minutes for the 15 mm spacing (top). Tissue contraction is evidenced by the greater inward electrode displacement for longer lesion times.

Ex Vivo Photographic Analysis

The digital photographic setup (Canon EOS 20D, Canon EF 100 mm f/2.8 Macro Lens, JPEG 3504×2336 pixels² Adobe Photoshop, Adobe Systems Incorporated, San Jose, CA, USA) is configured to normalize color and brightness across experiments and to effect high image contrast in the range of colors induced by heating each type of ex vivo media. Remote temperature probe measurements are used to facilitate interpretation of post-lesion photographs. A color-zone scheme, illustrated in Figure 4, is produced by quantizing the RGB pixel values of each photograph into four classes based on a heuristic assessment of tissue quality. For each 3-minute lesion, the final reading from each remote temperature probe is matched to the color zone where its thermocouple appears in the post-lesion photograph. These matches determine the distribution of temperature values associated with each color zone, and thus, with photographic appearance. Lesions dimensions are measured based on the outer limits the moderated-cooked color zone (yellow), which was found to reliably indicate temperatures greater than 50°C.

Sources of error in the derived photograph-to-temperature correspondence may include variation in tissue and photographic characteristics, imprecision in thermocouple location relative to color zone, displacement of cannulae and temperature probes during manipulation of the top tissue slab, spatial variation in time-integrated thermal exposure, and variation in heuristic assessment of color zone. In spite of these possible sources of error, the temperature distributions associated with each color zone are substantially unimodal, and their modal values increase in the order expected based on their appearance (Figure 4D). The regularity of these results is consistent with the interpretation that tissue appearance is indicative of the thermal exposure. It was not deemed necessary to match photographic appearance to the time-integrated thermal exposure, eg, Arrhenius cumulative thermal damage,¹² since a thermal damage factor is not substantially more informative than the temperature at 3 minutes when the lesion has already reached a pseudo-steady-state.

In Vivo Temperature Measurement

The clinical work related to this publication was conducted in adherence with Good Clinical Practice standards, and was reviewed by the IRB committee at the University of Massachusetts' Memorial Hospital (Worcester, MA, U.S.A.).

Data from bipolar lesions created in vivo are collected in the course of palisade treatment of SIJ pain, which employs a row of contiguous bipolar RF lesions to ablate the dorsal sacral innervations of the SIJ. For each of eight patients (age/sex: 48/F, 54/F, 54/M, 67/F, 79/F, 49/F, 46/M, 51/M) who presented with unilateral SIJ pain (positive physical exam with tenderness to SIJ palpation and positive resolution of pain for at least 1 week following SIJ block with 2 mL bupivacaine 0.25% and 2 mL triamcinolone 40 mg/ml), five to seven straight RF cannulae are placed in a line between the painful SIJ and the lateral aspects of the ipsilateral dorsal sacral foramina, starting superior to S1 and stopping inferior to S3. As shown in Figure 6, these cannulae are parallel, spaced by about 10 mm, and appear substantially perpendicular (ie, at a 90°, "right" angle) to the dorsal sacrum in a lateral fluoroscopic view. To achieve this, an AP fluoroscopic view is used to select a line for cannulae insertions that is lateral to the foramina and that is oriented substantially craniocaudally. Local anesthetic is injected into the skin along this line. The first cannula is lowered into the dorsal sacral periosteum under lateral fluoroscopic guidance, so that it appears perpendicular to the dorsal sacrum at the level of S2. Since the skin is not parallel to the sacrum, this cannula's hub is tilted cranially. To avoid the Ilium, the cannula's hub may be tilted slightly medially. Additional cannulae are placed above and below the first cannula. A ruler is held perpendicular to the first cannula as shown in Figure 6D, and the second cannula is positioned parallel to and 10 mm away from the first, for the purpose of determining the second cannula's point of skin insertion. All cannulae are lowered into the sacral periosteum under lateral fluoroscopic guidance to ensure that they are parallel to each other. A final AP image confirms their placement lateral of the dorsal sacral foramina. Placing cannulae in this manner tends to minimize tip offsets (see Figure 5D) and produce more complete inter-tip lesions. An alternative skin-perpendicular approach, used for some patients, is more likely to produce large tip offsets and, thus, a less complete lesion zone (see Figure 7).

Each cannula has a straight sharp tip, 10 cm shaft length, 10 mm tip length, and 20 gauge diameter (Cosman CC101020). Two 10 cm temperature-monitoring electrodes (Cosman disposable TCD-10 or autoclavable CSK-TC10) are connected to outputs 1 and 2 of a four-output radiofrequency generator (Cosman G4) configured for bipolar output. In regular practice, four electrodes can be connected to the generator and

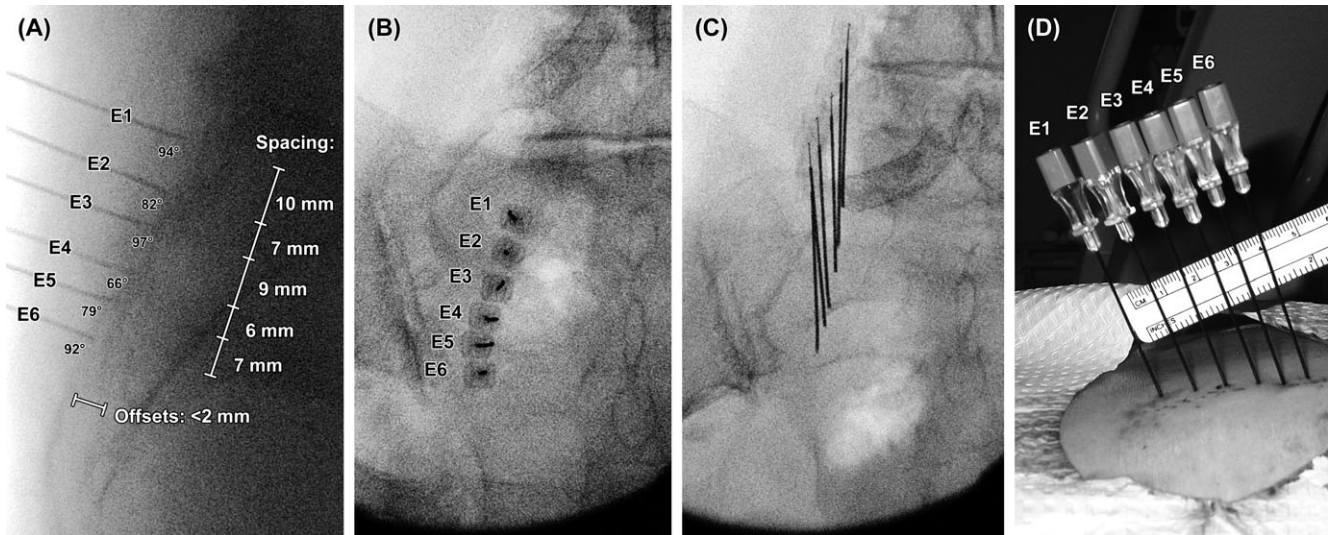


Figure 6. Palisade SIJ denervation performed by placing six straight RF cannulae of 20 gauge diameter and 10 mm tip length on a path between the S1, S2, and S3 dorsal sacral foramina and the ipsilateral SIJ, with a target parallel spacing of 10 mm. Bipolar lesions are produced between each pair of adjacent cannulae (E1–E2, E2–E3, E3–E4, E4–E5, and E5–E6) using a 90°C set temperature and 3-minute lesion time. The illustrated sacrum-perpendicular, parallel-cannulae approach produces smaller tip offsets than does the skin-perpendicular, parallel-cannulae approach shown in Figure 7, because the former approach targets sacrum-to-cannula angles that are closer to perpendicular (90°). (A) Lateral view. Electrode-to-surface angles are estimated relative to lines connecting the distal ends of the cannulae, which are in contact with the sacral surface. (B) Needle view. (C) AP view. (D) External view.

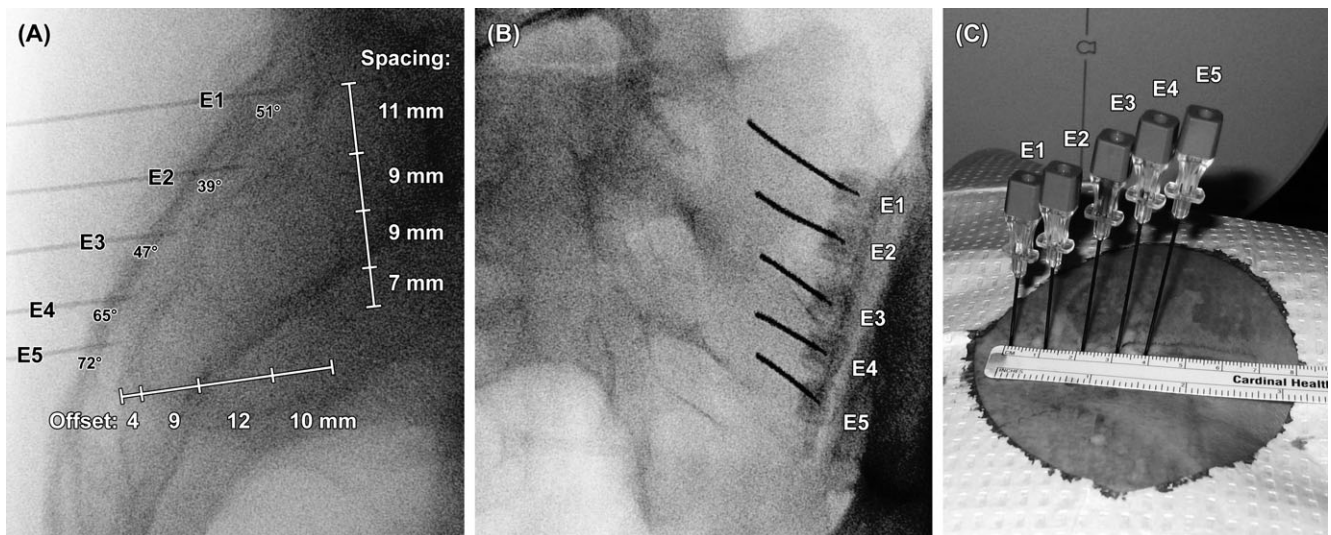


Figure 7. An alternative, skin-perpendicular palisade approach results in larger offsets between adjacent electrode tips than does the sacrum-perpendicular palisade approach shown in Figure 6. (A) Lateral view. (B) AP view. (C) External view.

multiple bipolar pairs can be energized at once to substantially reduce the lesion time. Before RF is applied to any pair, the sensory and motor stimulation response is assessed for each adjacent pair of cannulae to check for undesired proximity to the sacral nerve roots, and local anesthetic (0.5 mL lidocaine 1%) is injected into each cannula. In regular practice, sensory stimulation can be omitted because lesions are generated between each pair

of adjacent cannulae irrespective of sensory response, in order that a long, continuous palisade lesion is formed. By leapfrogging electrodes between adjacent pairs of cannulae, four to six bipolar RF lesions are generated sequentially, each using a 90°C set temperature and 3-minute set time. Afterward, each cannula is injected with a local anesthetic (0.5 mL bupivacaine 0.25%) and a steroid (0.1 mL triamcinolone 40 mg/ml).

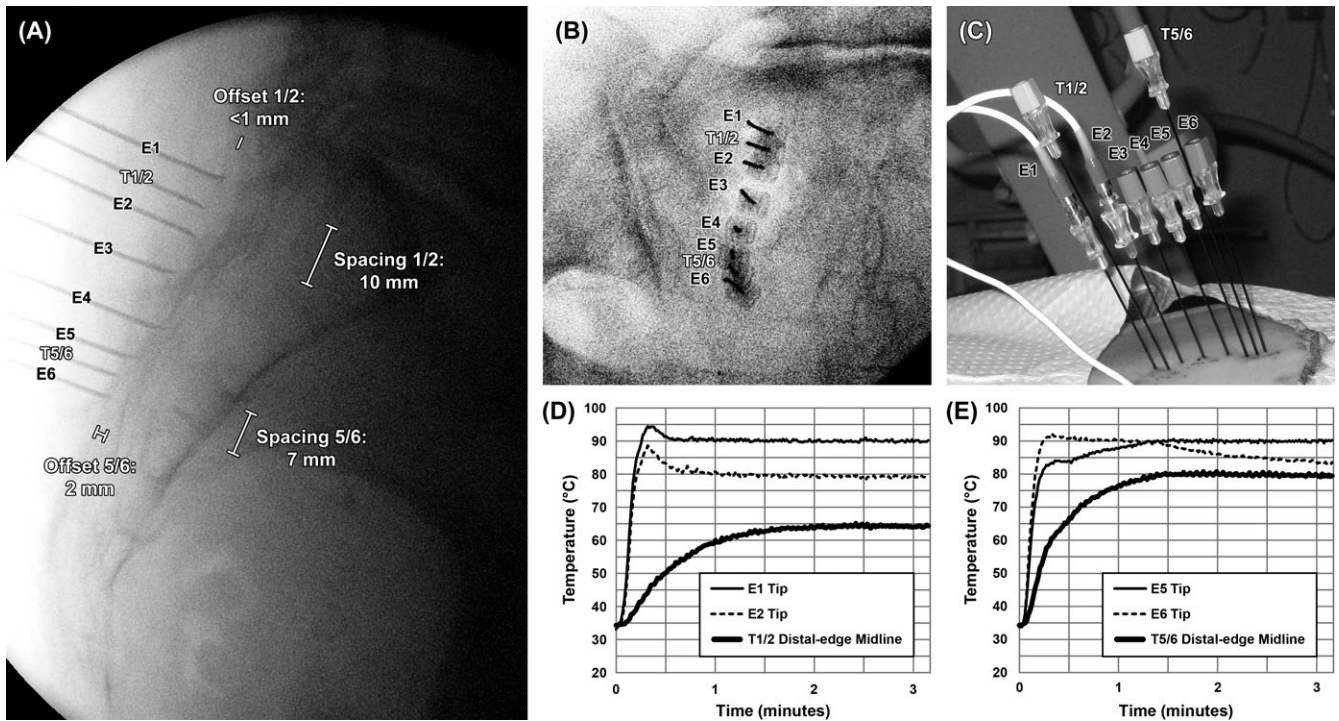


Figure 8. A row of electrodes (E1 to E6) and temperature probes (T1/2 and T5/6) is lowered into the dorsal sacral periosteum during clinical palisade treatment of SIJ pain. Probes T1/2 and T5/6 each house a thermocouple sensor located within 2 mm of its sharp distal end. They indicate sustained neurolytic temperatures at the sacral surface midway between bipolar pair E1–E2 and between bipolar pair E5–E6, which have 10 mm and 7 mm tip spacings, respectively. All electrodes have 20 gauge diameter and 10 mm tip lengths, and all bipolar pairs are energized using a 90°C set temperature and 3-minute lesion time.

For some bipolar lesions, a remote temperature probe is placed at the sacral surface midway between the two lesion cannulae to confirm that the inter-tip region achieves sustained neurolytic temperatures (Figure 8). Each remote temperature probe consists of a straight, 15-cm, 20-gauge cannula (Cosman CC15520) coupled with a disposable temperature-monitoring electrode (Cosman TCD-15) whose thermocouple lines are attached to output 3 of the G4 generator, with its RF line disconnected. Tip spacing, angle, and offset are estimated using external measurements and extrapolation from apparent cannulae diameters in lateral fluoroscopic images.

The ipsilateral L4 and L5 dorsal rami are each treated with a monopolar RF lesion using a 10-cm, 10-mm curved sharp tip, 20-gauge cannula (Cosman RFK-C101020S), set temperature 80°C, and set time 1.5 minutes. Before lesioning, each cannula placement is confirmed to demonstrate a sensory response to 50 Hz stimulation at 0.2 Volts, and no motor response to 2 Hz stimulation at 0.6 Volts. The same pre- and post-lesion injections are used as in the palisade treatment.

RESULTS

Ex Vivo Lesion Dimensions

For six bipolar lesions generated in different samples of adult bovine liver using 10 mm tip spacing, 20 gauge cannulae, 10 mm tip lengths, 90°C set temperature, and 3-minute lesion time, the average midline length was 12.52 mm with a standard deviation of 0.87 mm, and the average width was 15.06 mm with a standard deviation of 0.50 mm. As observed in a previous study,¹³ ex vivo RF lesion sizes in animal tissue do not exhibit large variations for identical setups. They also change smoothly as geometric and RF parameters are varied.

Figures 5, 9, and 10 show cross-sectional photographs of bipolar lesions produced in ex vivo bovine liver for a variety of configurations, and plot measurements of the cross-sectional midline length L and width W of the lesions' moderately-cooked regions (yellow color zone; see Figure 4). In particular, Figures 9 and 10 show the effect of variations in parallel tip spacing, tip diameter, and tip length for 90°C tip temperature and

3-minute lesion time. While the lesion width increases with increased tip spacing, the midline lesion length declines. The decline in width occurs over a wider range of spacing values when tip length and diameter are increased. Figure 5 shows the effect of variations in inter-tip angle, inter-tip parallel offset, set temperature, and lesion time, starting from the base configuration 10 mm parallel spacing, 20 gauge diameter, 10 mm tip length, 90°C tip temperature, 3-minute lesion time. In particular, the midline lesion length does not appear to decline precipitously for small inter-tip offsets and angles relative to the base configuration, which are likely to occur in actual clinical placements (Figure 5A, 5D, and 5E). For the base configuration, when the set temperature is 80°C or greater (Figure 5B), the entirety of the inter-tip region appears moderately or fully cooked (yellow or red color zone). For the base configuration, the lesion dimensions reach equilibrium between 2 and 3 minutes (Figure 5C). However, while 3 minutes is sufficient time for a lesion to reach its maximum extent in a variety of bipolar configurations relevant to pain management, for some other configurations, lesion times greater than 3 minutes can substantially increase inter-tip temperatures. In general, for smaller tip spacings, longer lesion times produce diminishing returns in terms of inter-tip tissue temperature (eg, compare the lesion at 3 and 5 minutes for the 15 mm spacing in Figure 5G). For larger tip spacings, longer lesion times can induce substantially higher temperatures in the inter-tip region, but the required lesion times may be considerably longer (eg, compare the lesion at 3 and 10 minutes for the 20 mm spacing in Figure 5G). For very large tip spacings where the electric field is not substantially focused in the inter-tip region, even a very long lesion time will not produce a connected lesion between tips.

The “Depth Cross Section” photograph in Figure 9 shows two examples of the cross-sectional depth dimension of a bipolar lesion, and Table 1 reports measurements of this dimension for various configurations. The midline lesion depth D follows a similar pattern of decline with increased tip spacing as does the midline lesion length L .

These results show that for bipolar configurations, the fraction of the inter-tip volume exceeding neurolytic temperatures (≥ 45 – 50°C) increases with decreased tip spacing, decreased tip offset, decreased inter-tip angle, increased tip length, increased cannulae diameter, increased tip temperature, and/or increased lesion time.

Ex Vivo Lesion Temperature Time Series

Figure 5F plots thermocouple temperatures measured at intra-tip and inter-tip locations during 3-, 5-, and 10-minute lesions in ex vivo bovine liver for the base configuration (defined above). While the tip temperatures reach steady-state in about 15 seconds, remote temperatures along the midline saturate only between 2 and 3 minutes, just as is illustrated photographically in Figure 5C. While the time between 2 and 3 minutes does not induce a substantial temperature increase, continuing the lesion after 2 minutes ensures that tissue temperatures exceed 45 – 50°C for a duration capable of inducing cell death,^{14–16} and reduces sensitivity to inter-tip spacing. For example, Figure 11 shows both slower and smaller temperature rises at corresponding inter-tip locations when the tip spacing is increased over the range 10 mm to 15 mm.

In Figures 5F, 8, and 11, the set temperature used was 90°C , but only one of the electrode tips in each bipolar pair achieves this temperature. This temperature disparity is common to bipolar RF both ex vivo and clinically because each electrode in a bipolar configuration serves as the voltage reference and path for return currents for the other electrode. As such, the same relative voltage and current waveform is applied to both electrodes, so only the higher tip temperature is regulated. The extent of the temperature disparity is determined by the relative electrode sizes and differences in tissue characteristics near each electrode’s tip. As such, the likelihood of disparity generally increases for larger tip spacings.

Other Ex Vivo Media

Bipolar lesion geometry appears quite similar in ex vivo animal muscle and bovine liver, as shown in Figure 11. The visible lesion in muscle roughly matches the moderately-cooked region in bovine liver (yellow color zone, $\geq 54.5^\circ\text{C}$). Also plotted in Figure 11 are direct measurements of temperatures at corresponding locations in muscle and liver lesions. The similarity of these temperature time-series suggests that relevant electro-thermal dynamics are similar in all these tissues, even though muscle starts changing color at a higher temperature than liver. Advantageously, ex vivo beef liver starts changing color between 45°C to 50°C , allowing photographic estimation of the entirety of the regions that reach neurolytic temperatures.

Lesions formed in egg white demonstrate substantial differences from those formed in solid animal tissue. Figure 12 compares ex vivo bipolar lesions in egg white

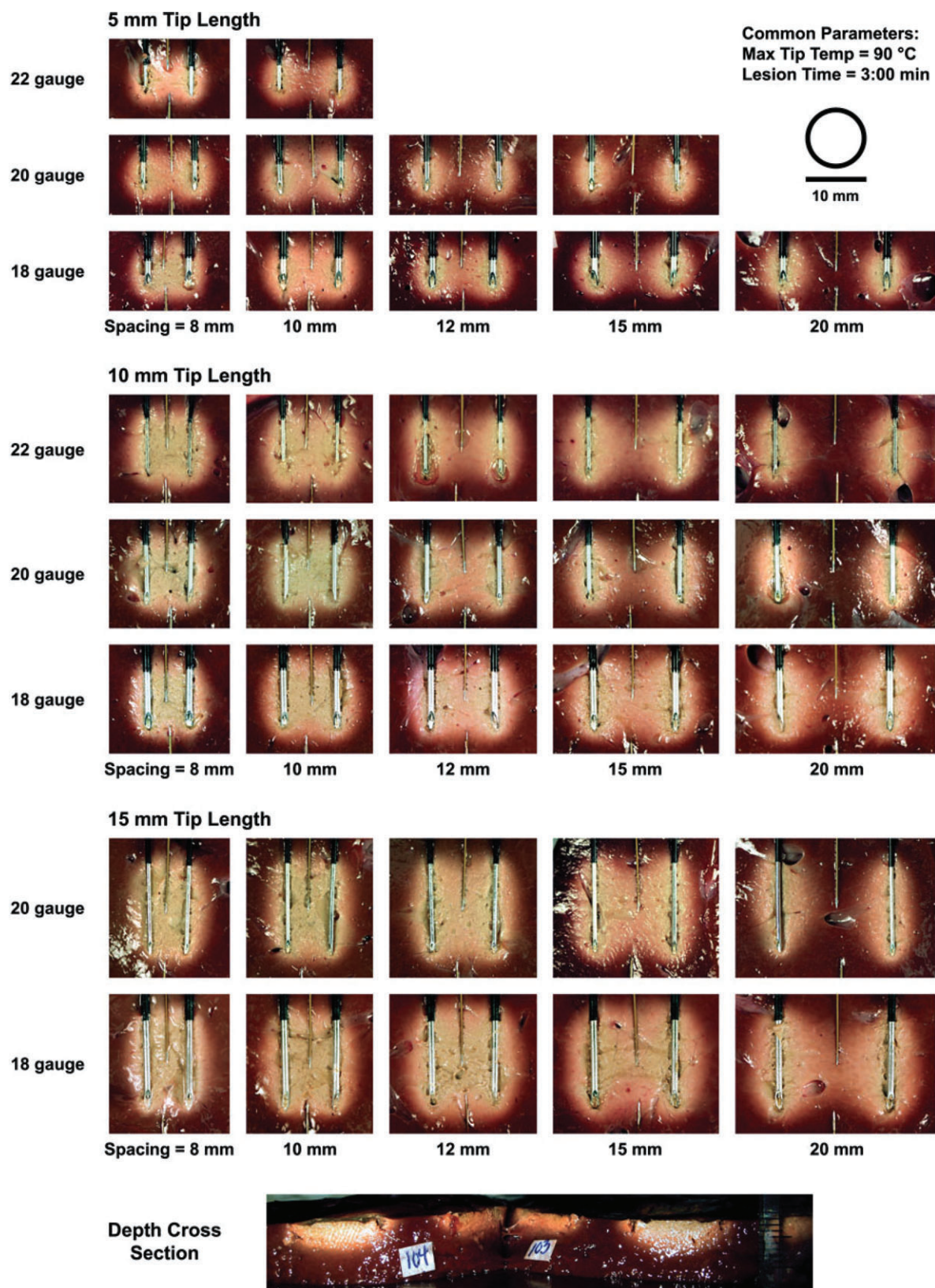


Figure 9. Cross-sectional photographs of bipolar lesions in ex vivo adult bovine liver show the lesion lengths L and widths W produced by different parallel tip spacings, tip diameters, and tip lengths, for 90°C tip temperature and 3-minute lesion time. The “Depth Cross Section” photograph shows two bipolar lesions in the lower liver slab, revealed by cutting the lower liver slab in a plane perpendicular to the tip lengths. Half of their midline depth dimension D can be measured in this manner (Table 1).

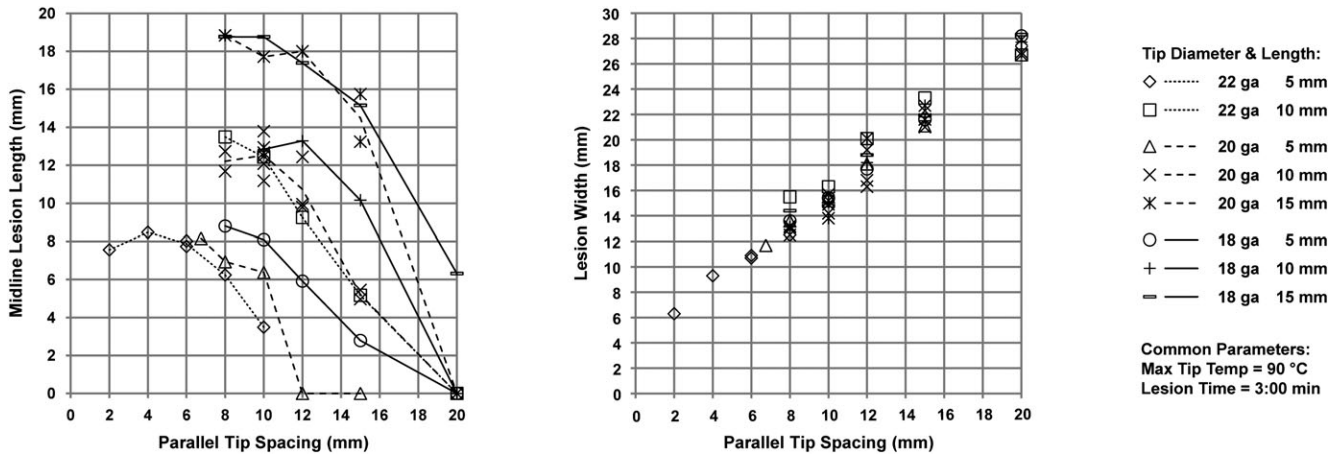


Figure 10. Measurements of midline lesion length L and width W in ex vivo adult bovine liver produced by a variety of parallel tip spacings, tip diameters, and tip lengths, for 90°C tip temperature and 3-minute lesion time, as photographed in Figures 9 and 12. (Left) The midline lesion length L increases with increased cannulae diameter and tip length. Line graphs connect the average midline lesion length over multiple runs of each tip spacing-diameter-length combination for the purpose of organizing the figure by tip diameter-length combinations; however, these lines do not necessarily indicate a linear trend in midline lesion length between larger spacings (eg, 15 and 20 mm) where the lesion splits into two parts around each tip. (Right) Lesion width is not strongly dependent on tip diameter or tip length.

Table 1. Ex Vivo Lesion Depth

Parallel Tip Spacing (mm)	Tip Diameter (ga)	Tip Length (mm)	Tip Temp. (°C)	Lesion Time (min : sec)	Midline Lesion Depth (mm)
10	20	10	90	3:00	8.1
10	18	10	90	3:00	8.8
10	18	5	90	3:00	5.3
20	20	10	90	3:00	0
20	20	15	90	10:00	5.6

The midline depth D of various parallel-tip bipolar lesions is based on bisection of the lower bovine liver slab as illustrated in the "Depth Cross Section" photograph of Figure 9.

and bovine liver using 22 gauge cannulae, 5 mm tip lengths, 90°C set temperature, and 3-minute lesion time. The egg white results match those reported in a previous study.¹¹ Whereas temperatures between bipolar electrode tips spaced by more than 6 mm do not appear substantially elevated in egg white, they are visibly raised in bovine liver. This apparent underestimation of lesion size in egg white may be due in part to the fact that egg white changes color only at 62–65°C.¹⁷ For example, in the egg-white lesion for 8 mm tip spacing shown in Figure 12, the remote probe's temperature increased from 28.1°C to 47.7°C, but the visible lesion did not contact the probe. However, egg white's high color-change temperature does not account for the fact that the proximal-edge midline temperatures in egg-white lesions were also 6°C to 14°C lower than those in the corresponding bovine liver lesions. Nor does it account for the fact that egg-white lesion shape is inconsistent across multiple experimental runs using the iden-

tical electrode setup, whereas lesions in bovine liver are consistently reproducible. These discrepancies may be explained by differences in the electrical, thermal, and mechanical properties of egg white fluid and solid animal tissue. In particular, spatial variations in egg white's constituents contribute to irregularities in heating patterns and color changes. For example, albumin protein density is variable and distributed irregularly within egg white. Because thermal denaturation of that protein causes first color changes, the visible lesion can be correspondingly variable and unpredictable. Furthermore, the other more fluid components of egg white have different thermal color-change characteristics and produce significant heat convection due to the absence of a cellular matrix. Convection, in which hotter, low-density fluid tends to rise, is evidenced by the top-heavy lesion shape that is typical in egg white. Convective flow during RF lesioning in egg white is visible microscopically, and is apparent

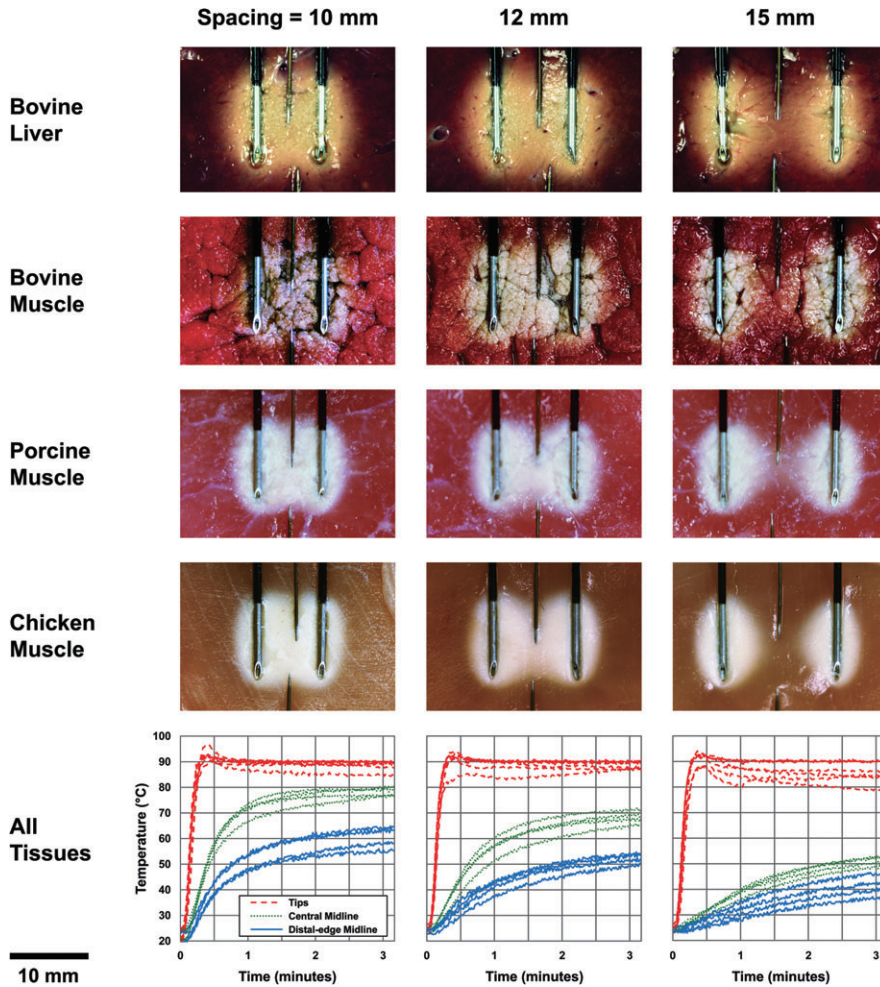


Figure 11. Cross-sectional photographs of bipolar lesions in ex vivo bovine liver, bovine muscle, porcine muscle, and chicken muscle. At each spacing, the electrode configuration is identical. Intra-tip and inter-tip temperatures for all tissues are plotted over the same time axis for each spacing. The midline temperatures decline with increased spacing. Configuration: variable spacing, 20 gauge diameter, 10 mm tip length, 90°C tip temperature, 3-minute lesion time.

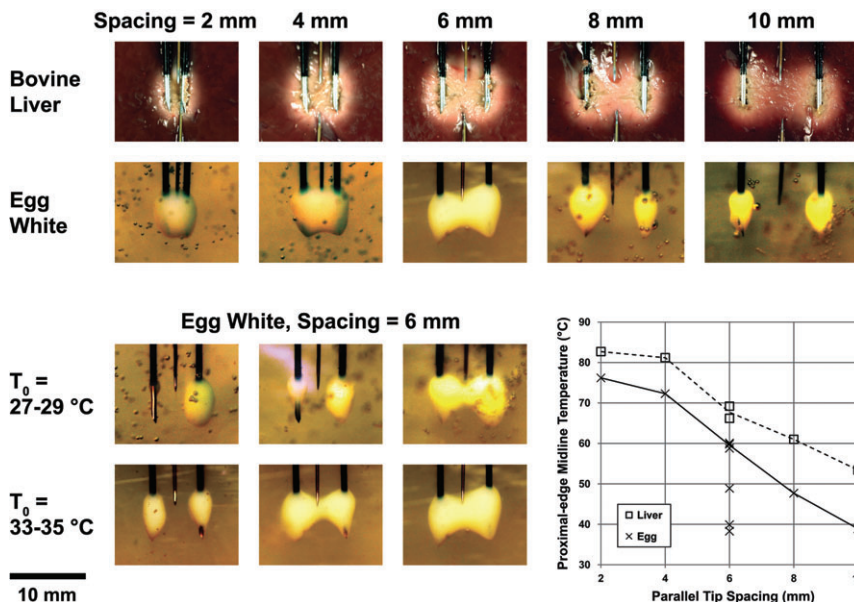


Figure 12. (Upper) Photographs of ex vivo bipolar lesions in egg white and adult bovine liver. At each spacing, the electrode configuration is identical. (Lower left) Repeated lesions in egg white using 6 mm tip spacing, with initial egg white temperatures T_0 ranging from 27–35°C. (Lower right) The final temperature at the proximal edge of the inter-tip midline for each of the lesions photographed. Line graphs connect the average temperatures for repeated runs of each spacing-media combination, omitting the disconnected egg white lesions at 6 mm spacing. The large variability in these temperatures across repeated runs at 6 mm spacing corresponds to the large variability in lesion shape shown at the lower left. Configuration: variable spacing, 22 gauge diameter, 5 mm tip length, 90°C tip temperature, 3-minute lesion time.

Table 2. In Vivo Temperature Measurements

Patient	Tip Spacing (mm)	Tip Offset (mm)	Time to 45°C (min : sec)	Time to 50°C (min : sec)	Steady State Temp. (°C)
A	5	7	0:07	0:08	82
B	7	2	0:10	0:13	80
B	10	0	0:20	0:30	64
C	10	1	0:20	0:30	60
D	10	4	0:11	0:17	62
C	11	0	0:32	0:55	53
D	12	2	0:24	0:35	62
A	9	14	1:19	N/A	49

In vivo temperature measurements were made near the sacral surface, halfway between bipolar electrodes, during clinical palisade treatment of SIJ pain (see Figure 8). Reported measurements were collected during the first lesion produced at both electrodes in each bipolar pair. Configuration: variable spacing, 20 gauge diameter, 10 mm tip lengths, 90°C set temperature, 3-minute lesion time.

macroscopically via movement of air bubbles. Heating egg white to 37°C before lesioning reduces convection but does not eliminate it. Convection dynamics, variability in lesion geometry, and inconsistency with animal-tissue lesion sizes raise substantial questions about the validity of egg white as an ex vivo media for modeling clinical RF lesion size.

In Vivo Lesion Temperature Time Series

During clinical palisade denervation of the SIJ in four patients, remote temperature probes were placed on the sacral surface near the distal-edge midlines of some electrode pairs. Measurements from these probes were used to ascertain whether sustained neurolytic temperatures (≥ 45 –50°C for more than 20 seconds^{14–16}) were achieved in the inter-tip region between electrode pairs, including the sacral surface. Figure 8 shows the setup for one patient. Table 2 documents that neurolytic temperatures above the 45°C to 50°C range are achieved at this position for parallel tip spacings up to 12 mm with 2 mm offset. These data are also consistent with an expected decrease in temperature at this position as tip spacing and offset increase.

Clinical outcomes are positive, but have so far only been assessed informally over a short time.

DISCUSSION

Bipolar Configuration Parameters

Previous conceptions about bipolar electrode spacing should be revised in light of the present study. First, the upper physical limit on bipolar electrode spacing is *not* 6 mm as reported by Pino et al.¹¹ That result was derived using an ex vivo egg white model which has substantially different physical properties from solid tissue, as detailed above. In the present study, in vivo temperature measurements demonstrated the generation of a “strip lesion” connecting bipolar electrode tips

spaced by as much as 12 mm. Ex vivo animal tissue experiments demonstrated the same effect for spacings as large as 20 mm. In both cases, these spacing values were the upper limits observed in this study, not the upper physical limit on bipolar electrode spacing. Larger tip spacings may be possible, but should be verified in vivo by inter-tip temperature monitoring before being put into regular clinical use.

Second, the tip spacing at which a bipolar thermal lesion transitions from a single volume into two volumes is not the same for all bipolar configurations. In the present study, ex vivo animal tissue experiments demonstrated that heating between bipolar tips is enhanced as tip diameter, tip length, tip temperature, and/or lesion time are increased (Figures 5, 9, and 10). That said, both ex vivo and in vivo data indicate that a parallel spacing of 10 mm is a conservative choice for the purpose of generating a rounded rectangular lesion (Figure 1B) using 10-mm or 15-mm tip lengths, 20- or 18-gauge cannulae, and 90°C set temperature, within a practical, 3-minute lesion time. For this configuration, lesion geometry appears to be fairly insensitive to small parameter variations, including spacing inaccuracies, inter-tip angles, and inter-tip offsets.

Table 3 outlines discussion of a number of geometric and RF parameters relevant to bipolar thermal lesion geometry.

Bipolar Lesion Size

Bipolar RF delivered between conventional RF cannulae can produce neurolytic temperatures over tissue volumes that are large by pain management standards. For example, as shown in Figure 10 and Table 1, a rounded rectangular lesion with length $L = 12$ mm, width $W = 15$ mm, and depth $D = 8$ mm can be created using a bipolar configuration with parallel tip spacing

Table 3. Discussion of Bipolar RF Configuration Parameters

Parameter	Discussion
Cannulae curvature	Parallel placement of straight cannulae by aligning shafts is uncomplicated. To maximize inter-tip heating when using curved cannulae, align their hub markings to reduce tip skew.
Relative tip size	Cannulae of the same tip length and diameter should be used. Differences in tip size will tend to produce a lower current density and lower temperatures at the larger tip.
Cannulae diameter	Increasing cannulae diameter (ie, decreasing gauge) enhances inter-tip lesioning, especially for larger tip spacings. 18 gauge cannulae improve inter-tip heating at spacings greater than 10 mm, but have a frontal cross-sectional area 193% that of 20 gauge cannulae, and thus cause greater insertion trauma. See Figures 9 and 10.
Tip length	For configurations that produce a lesion containing the entire inter-tip region, the midline lesion length can exceed the tip length by as much as 4 mm. To induce complete inter-tip lesioning, cannulae with 5 mm tips must be placed closer together than do those with 10 or 15 mm tips. See Figures 9 and 10.
Tip spacing	For 10 mm parallel spacing, the entirety of the inter-tip region can reach neurolytic temperature in a practical lesion time of 2 to 3 minutes. Inter-tip heating is not strongly sensitive to spacing in the range 8–12 mm for cannulae with 20- or 18-gauge diameter and 10- or 15-mm tip length. For spacings as large as 20 mm, preferential heating between electrode tips can be induced by means of greater tip length and diameter, longer lesion time, and/or higher tip temperature. See Table 1, and Figures 5, 9, and 10.
Tip offset	Minimizing offset (0 mm) maximizes inter-tip heating. As offset increases, lesion geometry transitions toward that of two monopolar lesions surrounding each tip separately. See Figure 5.
Tip angle	Minimizing angle (0° from parallel) maximizes the volume of an inter-tip lesion. Heating is focused where tips are closest since RF current follows the path of least resistance. See Figure 5.
Tip skew	Skew refers to two cannulae tips not falling in the same plane. For example, tip skew can arise when the shafts of two curved cannulae are parallel, but their tips are not. Skew is not explored in the present study, but will reduce inter-tip lesion cross section.
Tip temperature	A higher set temperature increases lesion size. A 90°C set temperature produces maximal lesions with 10°C buffer from boiling. A set temperature between 80 and 90°C may produce similar lesion sizes, with less risk of boiling for very small tip spacings in which the maximum temperature is located between the bipolar tips. See Figure 5.
Lesion time	Increasing lesion time improves the likelihood that the entirety of the inter-tip region will achieve sustained neurolytic temperatures (ie, exceeding 45°C to 50°C for more than 20 seconds ^{14–16}). Lesion times between 2 and 3 minutes can be used for 10 mm tip spacing and a 90°C set temperature, but at the lower end of that time range, the lesion size is more sensitive to misalignments between electrodes. See Figures 5, 9, 10 and 11.

$s = 10$ mm, tip length $l = 10$ mm, cannulae diameter $d = 20$ or 18 gauge, set temperature $T = 90^\circ\text{C}$, and lesion time $t = 3$ minutes. Using tip length $l = 15$ mm increases the rectangular lesion length to $L = 18$ mm. Using tip spacing $s = 12$ mm increases the rectangular lesion width to $W = 17$ mm.

In contrast, a monopolar RF electrode of 10 mm tip length, 20 or 18 gauge diameter, heated to 80°C to 90°C for 1.5–3 minutes, produces a roughly prolate-ellipsoidal lesion with semi-axes $L = 12$ –14 mm and $W = D = 5$ –8 mm in ex vivo adult beef liver (not pictured in this publication). Three such monopolar lesions are required to approximate the volume of a bipolar lesion created using only two electrodes of the same size, spaced by 10 mm (see Figure 13C). Extrapolating this to the situation where $N \geq 2$ electrode placements are arranged to form a bipolar RF palisade, roughly twice as many electrode placements ($2N-1$) would be required to create the same aggregate lesion zone if monopolar RF were used instead.

The size of conventional bipolar RF lesions can also exceed that of monopolar cooled RF lesions as applied in pain management. For example, it has been reported that a cooled RF electrode of 18 gauge diameter and

4 mm tip length (inserted through 17 gauge introducer cannulae) creates spherical lesions with diameter $L = W = D = 8$ –10 mm when heated to 60°C over 3 minutes (0.5 minutes pre-cooling plus 2.5 minutes heating).^{18–20} While much larger lesions of 30 to 50 mm diameter can be created using the cooled RF electrodes invented for tumor ablation in large organs by Professor Eric Cosman, Sr. in the 1990s (Radionics Cool-Tip RF System, Burlington, MA, U.S.A.),^{21–24} lesions of that size have not been suggested for use in the spinal pain management. The proximity of target nerves to non-target nerves, blood vessels, and the skin surface imposes an upper bound on the safe size of any heat lesion in the spine, whether produced by cooled or conventional RF. Uncertainty in cooled RF temperature control may additionally limit the use of larger cooled RF lesions near sensitive spinal structures. Since the maximum tissue temperature of a cooled RF lesion occurs at a variable distance from the electrode's tip, a remote temperature sensor placed at a fixed distance from the tip may not measure that maximum. For example, in vivo and ex vivo experiments have shown that tissue can reach 75°C within a cooled RF lesion when the electrode's remote tip sensor reads 60°C .^{18,20}

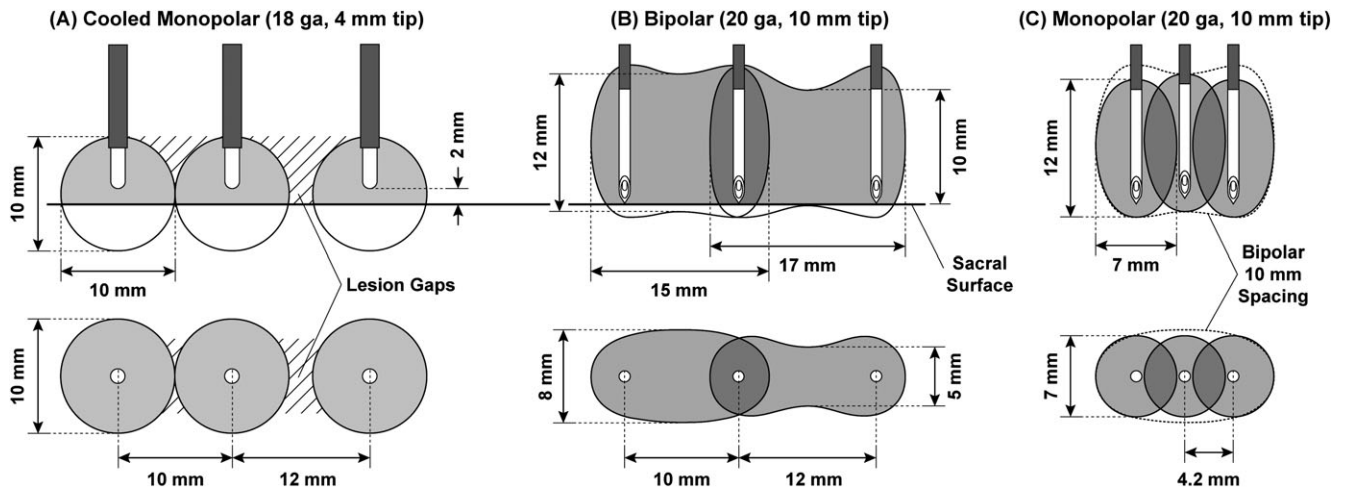


Figure 13. (A) Cooled monopolar lesion geometry for 10 and 12 mm tip-to-tip spacings, 2 mm tip-to-sacrum distance, 60°C set temperature, and 3-minute lesion time (0.5 pre-cooling + 2.5 heating).^{18–20} Gaps between and around adjacent lesions situated near the sacral surface can arise from small increases in tip-to-tip and tip-to-sacrum distances. (B) Bipolar lesion geometry for 10 mm and 12 mm tip-to-tip spacings, 0 mm tip-to-sacrum distance, 90°C set temperature, and 3-minute lesion time. Individually, bipolar lesions can be larger than both cooled and noncooled monopolar lesions. When arranged in a palisade on the sacral surface, bipolar lesions can collectively produce a lesion zone of consistent height, width, and depth that has fewer gaps than the lesion zone produced by the reported cooled RF SIJ method. (C) Three monopolar lesions, created using 90°C set temperature and 3-minute lesion time, are required to approximate a single bipolar lesion for 10 mm tip spacing and the same RF parameters (shown by the dotted outline). (A–C) Each panel shows a set of thermal lesions in both lateral (top) and needle (bottom) views.

In contrast, the maximum temperature during conventional monopolar and bipolar RF lesioning can be directly measured and controlled since it has a known position, either within the electrode tip(s), or within the inter-tip region for unusually small bipolar spacings. As a technique for creating larger lesions in nerve tissue, cooled RF also has a number of practical disadvantages relative to conventional bipolar RF. The diameters of current cooled electrodes are relatively large to accommodate an internal water cooling system, and thus, cooled electrodes can cause greater insertion trauma. For example, a 17-gauge cooled RF introducer has a frontal cross-sectional area which is $(1.47 \text{ mm}/1.27 \text{ mm})^2 = 134\%$ that of an 18-gauge conventional cannula, and $(1.47 \text{ mm}/0.9144 \text{ mm})^2 = 258\%$ that of 20-gauge conventional RF cannula. Cooled electrodes are currently for single use only, and each one costs about 10 times more than two conventional electrodes and cannulae per procedure.

Currently available reports on the size of cooled bipolar RF lesions are not comparable to the present study because they relate only to lesioning within the confined space between spinal vertebrae.^{25–27} Nevertheless, it can be said that the safe use of cooled bipolar RF in the spine is limited by the same size constraints that govern all RF methods, and by the same temperature-control uncertainties as monopolar cooled RF.

The great variety in available sizes of inexpensive RF cannulae, and the inherent adjustability of bipolar electrode/cannulae spacing, permit diverse sizing and shaping of conventional bipolar lesions, both to ablate target anatomy and to avoid nontarget anatomy. Figures 5 and 9 show many examples of this conformal flexibility, by which lesion width can be adjusted nearly independently of lesion length and depth. In contrast, monopolar RF applied to a cylindrical electrode is restricted to producing axially-symmetric lesions, where lesion width equals lesion depth.

Palisade Sacroiliac Joint Pain Treatment

Dorsal innervation of the SIJ has been reported to include the L4 and L5 dorsal rami, and the S1, S2, S3, and sometimes S4 lateral branches.^{1,2} Recent literature reviews contain numerous approaches to the treatment of chronic back pain by radiofrequency ablation of dorsal SIJ innervation.^{1,28,29} Typically, lesioning of the L4 and L5 dorsal rami is accomplished using conventional monopolar RF since these nerves have regular locations relative to bony landmarks. Approaches differ in their methods for lesioning the sacral lateral branches, which do not have a stereotyped location relative to bony landmarks. These nerves have been reported to follow branching, irregular pathways between the lateral aspect of the dorsal sacral foramina and the dorsal SIJ

line, ranging from points slightly superior to S1 to those slightly inferior to S3.² Conventional monopolar RF and pulsed RF methods use electrical stimulation to guide electrode placement near individual lateral branches of the dorsal sacral rami.^{2,30–33} These techniques have the advantage of targeting nerves specifically, but may miss some nerve branches without exhaustive search and concomitant tissue trauma. Conventional bipolar RF has been used to target either the SI joint itself,³ or the sacral lateral branches as they emerge from the S1–S3 foramina.⁴ These bipolar RF methods take advantage of the absence of motor function in the sacral lateral branch nerves by using larger lesions to ablate the likely locations of multiple nerves at once, thereby avoiding the complication of sensory-stimulation-based search. Similarly, monopolar RF using internally-cooled RF electrodes has been employed to lesion the lateral branch nerves as they emerge from the S1–S3 foramina.^{18–20}

Reported outcomes for SIJ treatment by conventional and cooled RF have not yet proven a superior method. Cohen et al. suggest that the higher success rate of their cooled RF method relative to some conventional RF methods is due to the creation of larger lesions, but warn that this comparison is not statistically powered, and that the apparent improvement may be due to their use of stricter patient-inclusion criteria than those used in other studies.²⁰ Based on the results of the present study and careful analysis of the geometric and RF parameters reported in the literature (Table 4), it is conceivable that larger lesions were being created in the cooled RF studies than were in the previous bipolar RF studies. However, the present study also suggests that previous bipolar RF techniques can be improved to create larger lesions, with smaller inter-lesion gaps, and with fewer cannulae placements than the cooled RF method (Figure 13).

The bipolar palisade method of SIJ denervation proposes a number of adjustments to previously reported bipolar RF and cooled RF methods. First, electrode positions and RF parameters are selected to create bigger lesions, using conventional electrodes and cannulae (Table 4). Second, cannulae are placed on a straight line lateral to the sacral foramina, starting superior to S1 and ending inferior to S3 or S4 (Figures 2 and 6). Relative to perforaminal placements, this approach is configured to reduce difficulty in identifying the dorsal sacral apertures,¹⁹ to reduce the risk of damage to the sacral roots,^{18,19} and to reduce the number of cannulae placements required (palisade uses 5 to 7 placements;

Table 4. SIJ Treatment Parameters

Reference	RF Type	Targets	Electrode Trajectory	Number of Placements	Electrode Spacing (mm)	Electrode Diameter (ga)	Tip Length (mm)	Temp (°C)	Time Per Lesion (min)
Ferrante et al. ³	Bipolar	Long axis of the posterior SIJ	N/A	Unspecified	< 10	20 or 22	5 or 10	90	1:30
Pino et al. ¹¹	Bipolar	N/A	N/A	N/A	≤ 6	22	5	90	2:00–2:30
Burnham et al. ⁴	Bipolar	Surround lateral aspect of S1, S2, and S3	Perpendicular to skin, contact the sacrum.	12	4–6	20	10	80	1:30
Wright et al. ¹⁸	Monopolar, cooled	Surround lateral aspect of S1, S2, S3, and maybe S4	Perpendicular to skin, about 2 mm from the sacrum	8 or 9	≈ 10	18 (17 ga cannula)	4	60	2:30
Kapural et al. ¹⁹									
Cohen et al. ²⁰									
Palisade	Bipolar	A line lateral to S1, S2, S3, and maybe S4	Perpendicular to the sacrum, contact the sacrum	5, 6, or 7	8–12	20 or 18	10	90	3:00

Configurations for SIJ treatment using conventional bipolar RF and monopolar cooled RF. Cylindrical electrodes/cannulae of 22, 20, 18, and 17 gauge (ga) have 0.71, 0.91, 1.27, and 1.47 mm diameters, respectively.

periforaminal bipolar RF using 12 placements;⁴ and periforaminal cooled RF uses 8 to 9 placements^{18–20}). Third, cannula hubs are tilted cranially and placed substantially perpendicular to the dorsal sacrum, so that adjacent tips are parallel and aligned with minimal offset, angle, and skew. Fourth, a bipolar lesion is created between each adjacent pair of cannulae, and multiple bipolar lesions can be created at once using a suitable four-electrode RF generator. The objective is the generation of a single, continuous lesion zone spanning the entire region through which lateral branches travel from the sacral foramina to the ipsilateral SIJ (Figure 2). Each bipolar lesion is expected to ablate nerves in a strip ranging from the dorsal sacral surface to about 10 mm above it, and continuity is guaranteed between adjacent lesions that share a common central electrode (Figure 13B). In contrast, previous approaches only target the expected locations of lateral branch nerves, and may thus miss nerves at irregular locations and depths.¹⁹ The efficacy of the palisade method must ultimately be determined by formal study of clinical outcomes. However, clinical work so far has shown that the method is uncomplicated, can be performed in less than an hour, and produces positive short-term results.

A principal difficulty in using monopolar cooled RF for either palisade or periforaminal electrode arrangements is the selection of tip-to-tip and tip-to-sacrum distances that will reliably avoid gaps in the final aggregate lesion zone. This difficulty is intrinsic to the spherical shape of the individual lesions, as illustrated in Figure 13A. For a cooled monopolar electrode configured to produce a spherical lesion with 8–10 mm diameter, the electrode's sequential positions must be spaced by no more than 8–10 mm to avoid gaps between adjacent lesions. Furthermore, as the spacing is increased toward that upper limit, the distance between the electrode and the sacral surface must be targeted with increased accuracy to avoid gaps between the sacral surface and points of lesion overlap. Satisfying these constraints increases the number of required lesions, reduces ablation of nerves traveling at different distances from the sacral surface, and/or damages a larger volume of healthy bone. Even then, gaps can still arise between adjacent lesions if the actual tip-to-tip or tip-to-sacrum distances differ by small amounts from those intended. In contrast, conventional bipolar lesion geometry is less sensitive to tip-to-tip targeting inaccuracies, and there is no uncertainty about tip-to-sacrum distances because conventional RF cannulae are placed in direct contact with the sacral surface (see Figure 13B).

Since at least one report on the cooled RF method estimates a spacing of 10 mm between adjacent electrode positions, and a distance of 2 mm between the electrode's tip and the sacral surface, it is conceivable that nerve-sparing, inter-lesion gaps contributed to some patients' nonresponse to that treatment.¹⁹ This issue may not be resolved simply by increasing the diameter of spherical cooled RF lesions. Doing so would also increase the lesion dimension lateral to the line connecting individual lesions, and thereby increase the risk of injury to the sacral nerve roots.^{18,19} Indeed, based on *in vivo* temperature measurements at the posterior sacral foraminal aperture (PSFA) during cooled RF lesioning using parameters expected to produce a lesion with 8–10 mm diameter, Wright et al. urge caution in placing a cooled RF probe “less than 7 mm from the PSFA to avoid heating the spinal nerve to neurodestructive temperature.”¹⁸

Published studies of cooled bipolar RF lesion geometry are currently too limited to motivate its application in SIJ treatment, both because the lateral/depth dimension of these lesions has not yet been mapped to assess risk to sacral nerve roots, and because the reported lesion times are very long (13–20 minutes) for large, nonparallel tip spacings (20.9–38.6 mm).^{25–27} Similarly long lesion times enable conventional bipolar RF to produce a strip lesion for large parallel tip spacings without substantially increasing either the midline or the overall lateral/depth dimension of the lesion (eg, 20 mm tip spacing, 10-minute lesion time; see Figure 5G and Table 1). The cooled RF method, in both bipolar and monopolar forms, also has a number of practical disadvantages, including the use of a 17-gauge cannulae that increases placement trauma, the need to manage a cool-water pumping system, the complication of switching between conventional and cooled RF equipment to treat L4-L5 and S1-S3,²⁰ and a drastically higher per-procedure equipment cost.

The technical observations in this paper are provided to assist clinicians in refining RF methods for SIJ treatment, whether for palisade or periforaminal electrode arrangements. The bipolar palisade technique presented in Figures 2 and 6 is engineered in accordance with the working theory that a larger lesion zone over the dorsal sacrum can improve the degree and duration of SIJ-related pain reduction,²⁰ and with the objective of minimizing acute trauma, reducing procedural complications, and moderating treatment costs. Nevertheless, several variants of the presented method are worthy of mention. For example, it may be advantageous to use

18-gauge cannulae rather than 20-gauge cannulae. Since 18-gauge cannulae allow somewhat larger inter-tip spacings (see Figures 9 and 10), the same aggregate palisade width could be produced either with fewer total cannula insertions or with shorter 5-mm tip lengths, to moderate unnecessary damage to healthy tissue. Similarly, since 18-gauge bipolar lesions extend somewhat farther distally to the inter-tip region, they may better heat inter-tip depressions in the sacral surface, which could plausibly harbor nerves in both bipolar RF and cooled RF approaches. On the other hand, an 18-gauge cannula produces greater insertion trauma, since its frontal cross-sectional area is $(1.27 \text{ mm} / 0.9144 \text{ mm})^2 = 193\%$ that of a 20-gauge cannula. In another procedural variant shown in Figure 7, electrodes are inserted perpendicular to the skin and at an acute angle to the sacrum, rather than perpendicular to the sacrum, as shown in Figure 6. This variant has also produced positive short-term clinical results, and it could be argued that it uses fewer cannulae to cover the same distance along sacral surface. However, acute angles between cannulae and the sacrum produce larger tip offsets that may lead to an incomplete lesion zone. Another variant, not explored in this study, involves placing each cannula exactly perpendicular to the sacrum by allowing a small angle between adjacent cannulae. This could have the advantage of reducing tip offsets for sacra with high curvature, but may complicate the targeting of inter-tip spacings.

Other Applications

The size and shape of bipolar RF lesions may be advantageous in other pain management applications where larger lesions are desired, or where it is desired to place lesions side-by-side without gaps. Since the width and length of bipolar lesions can be independently adjusted by varying the inter-electrode spacing and tip length, they may be useful to target nerves that have atypical location relative to bony landmarks, and which may also be proximate to sensitive structures. For example, bipolar lesions could be employed to reduce the number of cannula positions required by methods of medial branch neurotomy that utilize multiple, closely-spaced monopolar lesions to create a larger aggregate lesion zone.^{34,35} In particular, one might efficiently lesion a medial branch nerve at a mid-thoracic level (T5–T8) by placing bipolar electrodes on opposite sides of the inter-transverse region within which the nerve's location exhibits high inter-patient variability.³⁶ Conventional bipolar RF could also be reconsidered for intradiscal RF

heating, since the present study suggests that a longer lesion time can produce substantial inter-tip heating at larger tip spacings that previously thought.

Model Validity

Ex vivo tissue has long been used to assess RF lesion geometry^{6,10,11,13,20,25–27,35} and is an important tool for multifactor assessment of RF lesion geometry to guide development of clinical protocols. The results of such ex vivo studies, whether using human or animal tissue, must always be delivered with the caveat that they are biased by postmortem changes in cellular physiology, interstitial fluid, and blood flow. Other differences from the clinical context include pre-lesion tissue temperature and tissue inhomogeneities, such as the presence of bone and large blood vessels. Since the effect of these differences has not yet been adequately quantified, lesion size in the present study was assessed conservatively using room-temperature tissue samples and measurements based on the moderately-cooked color zone (yellow), corresponding to temperatures higher than 45°C to 50°C, which is assumed to induce neurolysis clinically. Direct temperature measurements in the ex vivo lesion were used to calibrate tissue color changes that might otherwise be misleading about lesion size. Demonstration of consistent lesion size and direct temperature measurements across multiple animal tissue types were used to check the results' generality. Given uncertainties about any ex vivo model, the present study was focused on characterizing geometrical changes across a wide range of tissue parameters to frame the results of in vivo temperature mapping, rather than quantifying ex vivo lesion size statistically. Most importantly, in vivo temperatures measured during a clinical SIJ treatment were consistent with those measured ex vivo at corresponding locations in the inter-tip region.

REFERENCES

1. Cohen SP. Sacroiliac joint pain: a comprehensive review of anatomy, diagnosis and treatment. *Anesth Analg*. 2005;101:1440–1453.
2. Yin W, Willard F, Carreiro J, Dreyfuss P. Sensory stimulation-guided sacroiliac joint radiofrequency neurotomy: technique based on neuroanatomy of the dorsal sacral plexus. *Spine*. 2003;28:2419–2425.
3. Ferrante FM, King LF, Roche EA, et al. Radiofrequency sacroiliac joint denervation for sacroiliac syndrome. *Reg Anesth Pain Med*. 2001;26:137–142.

4. Burnham RS, Yasui Y. An alternate method of radiofrequency neurotomy of the sacroiliac joint: a pilot study of the effect on pain, function, and satisfaction. *Reg Anesth Pain Med.* 2007;32:12–19.
5. Cosman Sr ER, Nashold BS, Ovelman-Levitt J. Theoretical aspects of radiofrequency lesions in the dorsal root entry zone. *Neurosurgery.* 1984;15:945–950.
6. Cosman Jr ER, Cosman Sr ER. Electric and thermal field effects in tissue around radiofrequency electrodes. *Pain Med.* 2005;6:405–424.
7. Sweet WM, Mark VH. Unipolar anodal electrolyte lesions in the brain of man and cat: report of five human cases with electrically produced bulbar or mesencephalic tractotomies. *Arch Neurol Psychiatry.* 1953;70:224–234.
8. Cosman BJ, Cosman Sr ER. *Guide to Radio Frequency Lesion Generation in Neurosurgery.* Burlington, MA: Radionics; 1974.
9. Cosman Sr ER, Cosman BJ. Methods of making nervous system lesions. In: Wilkins RH, Rengachary SS, eds. *Neurosurgery.* New York: McGraw-Hill; 1984:2490–2499.
10. Cosman Sr ER, Rittman WJ, Nashold BS, Makachinas TT. Radio frequency lesion generation and its effect on tissue impedance. *Appl Neurophysiol.* 1988;51:230–242.
11. Pino CA, Hoeft MA, Hofsess C, Rathmell JP. Morphologic analysis of bipolar radiofrequency lesions: implications for treatment of the sacroiliac joint. *Reg Anesth Pain Med.* 2005;30:335–338.
12. Haemmerich D, Webster JG, Mahvi DM. Thermal dose versus isotherm as lesion boundary estimator for cardiac and hepatic radio-frequency ablation. *Proceedings of the 25th Annual International Conference of IEEE EMBS;* 2003: 134–137.
13. Bogduk N, Macintosh J, Marsland A. A technical limitation to efficacy of radiofrequency neurotomy for spinal pain. *Neurosurgery.* 1987;20:529–535.
14. Brodkey JS, Miyazaki Y, Ervin FR, Mark VH. Reversible heat lesions with radiofrequency current: a method of stereotactic localization. *J Neurosurg.* 1964;21:49–53.
15. Dieckmann G, Gabriel E, Hassler R. Size, form, and structural peculiarities of experimental brain lesions obtained by thermocontrolled radiofrequency. *Confin Neurol.* 1965;26:134–142.
16. Smith HP, McWhorter JM, Challa VR. Radiofrequency neurolysis in a clinical model. Neuropathological correlation. *J Neurosurg.* 1981;55:246–253.
17. Yang S-C, Baldwin RE. Functional properties of eggs in foods. In: Stadelman WJ, Cotterill OJ, eds. *Egg Science and Technology.* Binghamton, NY: Haworth Press; 1995.
18. Wright RF, Wolfson LF, DiMuro JM, Peragine JM, Bainbridge SA. In vivo temperature measurement during neurotomy for SIJ pain using the Baylis SInergy probe. *International Spine Intervention Society 15th Annual Scientific Meeting;* 2007: 82–84.
19. Kapural L, Nageeb F, Kapural M, Cata JP, Narouze S, Mekhail N. Cooled radiofrequency system for the treatment of chronic pain from sacroiliitis: the first case-series. *Pain Pract.* 2008;8:348–354.
20. Cohen SP, Hurley RW, Buckenmaier III CC, Kurihara C, Morlando B, Dragovich A. Randomized placebo-controlled study evaluating lateral branch radiofrequency denervation for sacroiliac joint pain. *Anesthesiology.* 2008; 109:279–288.
21. Goldberg SN, Gazelle GS, Solbiati L, Rittman WJ, Mueller PR. Radio-frequency tissue ablation: increased lesion diameter with a perfusion electrode. *Acad Radiol.* 1996; 3:636–644.
22. Lorentzen T. A cooled needle electrode for radio-frequency tissue ablation: thermodynamic aspects of improved performance compared with conventional needle design. *Acad Radiol.* 1996;3:556–563.
23. Solbiati L, Goldberg SN, Ierace T, et al. Hepatic metastases: percutaneous radio-frequency ablation with cooled-tip electrodes. *Radiology.* 1997;205:367–373.
24. Goldberg SN, Solbiati L, Hahn PF, et al. Large-volume tissue ablation with radio frequency by using a clustered, internally cooled electrode technique: laboratory and clinical experience in liver metastases. *Radiology.* 1998; 209:371–379.
25. Pauza K. Cadaveric intervertebral disc temperature mapping during disc biacuplasty. *Pain Physician.* 2008;11: 669–676.
26. Petersohn JD, Conquergood LR, Leung M. Acute histologic effects and thermal distribution profile of disc biacuplasty using a novel water-cooled bipolar electrode system in an in vivo porcine model. *Pain Med.* 2008;9:26–32.
27. Kapural L, Ng A, Mekhail N, Nicks D. Histological changes and temperature distribution studies of a novel bipolar radiofrequency heating system in degenerated and nondegenerated human cadaver lumbar discs. *Pain Med.* 2008;9:68–75.
28. Hansen HC, McKenzie-Brown AM, Cohen SP, et al. Sacroiliac joint interventions: a systematic review. *Pain Physician.* 2007;10:165–184.
29. Rupert MP, Lee M, Manchikanti L, Datta S, Cohen SP. Evaluation of sacroiliac joint interventions: a systematic appraisal of the literature. *Pain Physician.* 2009;12: 399–418.
30. Gevarguez A, Groenemeyer D, Schirp S, Braun M. CT-guided percutaneous radiofrequency denervation of the sacroiliac joint. *Eur Radiol.* 2002;12:1260–1365.
31. Cohen SP, Abdi S. Lateral branch blocks as a treatment for sacroiliac joint pain: a pilot study. *Reg Anesth Pain Med.* 2003;28:113–119.
32. Buijs EJ, Kamphuis ET, Groen GJ. Radiofrequency treatment of sacroiliac joint-related pain aimed at the first three sacral dorsal rami: a minimal approach. *Pain Clinic.* 2004;16:139–146.

33. Vallejo R, Benyamin RM, Kramer J, Stanton G, Joseph NJ. Pulsed radiofrequency denervation for the treatment of sacroiliac joint syndrome. *Pain Med.* 2006;7:429–434.
34. Aprill C, Bogduk N, Dreyfuss P, et al. *Practice Guidelines for Spinal Diagnostic and Treatment Procedures*. San Francisco, CA: International Spine Intervention Society; 2004.
35. Derby R, Lee CH. The efficacy of a two needle electrode technique in percutaneous radiofrequency rhizotomy: an investigational laboratory study in an animal model. *Pain Physician.* 2006;9:2707–2214.
36. Chua WH, Bogduk N. The surgical anatomy of thoracic facet denervation. *Acta Neurochir (Wien).* 1995;136:140–144.